Supplementary Information

Cellulose Acetate Composites with Bamboo Cellulose Nanofibers: Crystallinity Preservation during Tetrabutylammonium Salt-Catalyzed Surface Acetylation

Hao Wang,[a] Kyoya Shirotani,[a] Naoki Wada,[b] Kenji Takahashi[b]

[a]*Graduate School of Natural Science and Technology, Kanazawa University, Japan*

[b]*Institute of Science and Engineering, Kanazawa University, Kanazawa, Japan*

1. Effects of TBA-based salts on CNF crystallinity

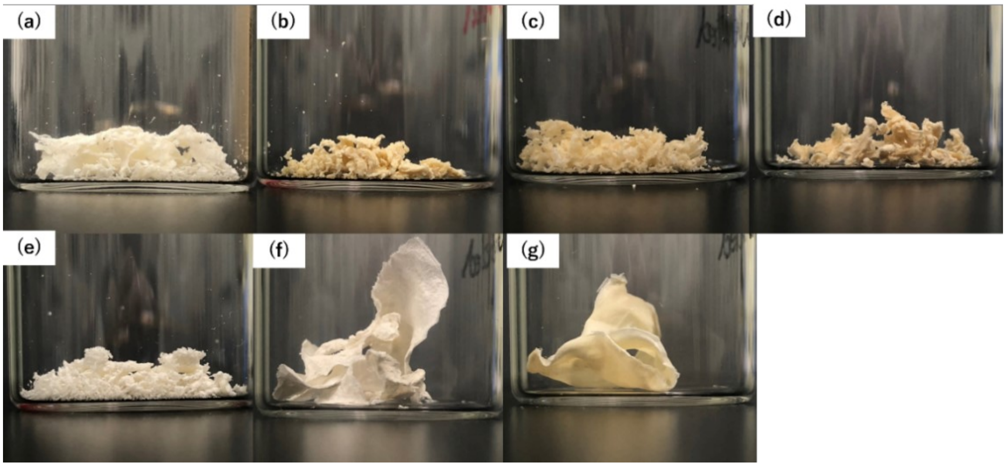

Figure S1. Images of regenerated bamboo CNFs. (a) TBA-acetate, (b) TBA_2-succinate, (c) TBA_2-oxalate, (d) TBA_2-malonate, (e) TBA_2-fumarate, (f) TBA_2-maleate, and (g) TBA_3-citrate.

2. Determination of the degree of substitution of CNF-ac

To clarify the determination of the degree of substitution (DS), note that CNF acetylation was conducted under heterogeneous reaction conditions. In the employed solvent system, CNFs were not fully dissolved; consequently, acetylation occurred predominantly at the accessible surface hydroxyl groups of CNFs. Therefore, a DS value of 0.5 does not imply homogeneous substitution of 1/6 of all hydroxyl groups along the cellulose chains. Instead, the majority of the cellulose backbone (estimated to exceed 80%) remained essentially unmodified and retained its native cellulose structure. This limited surface substitution also explains why the obtained CNF-ac remained insoluble in common organic solvents.

To accurately determine the DS of the initially introduced acetate groups by NMR spectroscopy, the remaining unreacted hydroxyl groups must be further derivatized without altering the pre-existing acetate moieties. Accordingly, the residual –OH groups were converted into ester groups via benzoylation, thereby increasing the overall DS and rendering the material soluble in organic solvents suitable for NMR analysis. Importantly, the characteristic NMR signals of benzoate groups are well separated from those of acetate groups, enabling unambiguous quantification of the acetate DS. Thus, the secondary benzoylation step serves as an analytical strategy to enable reliable DS determination of CNF-ac produced via heterogeneous surface acetylation, rather than as a modification intended to alter the original acetate structure. The benzoylation reaction mechanism is shown in Scheme S1.

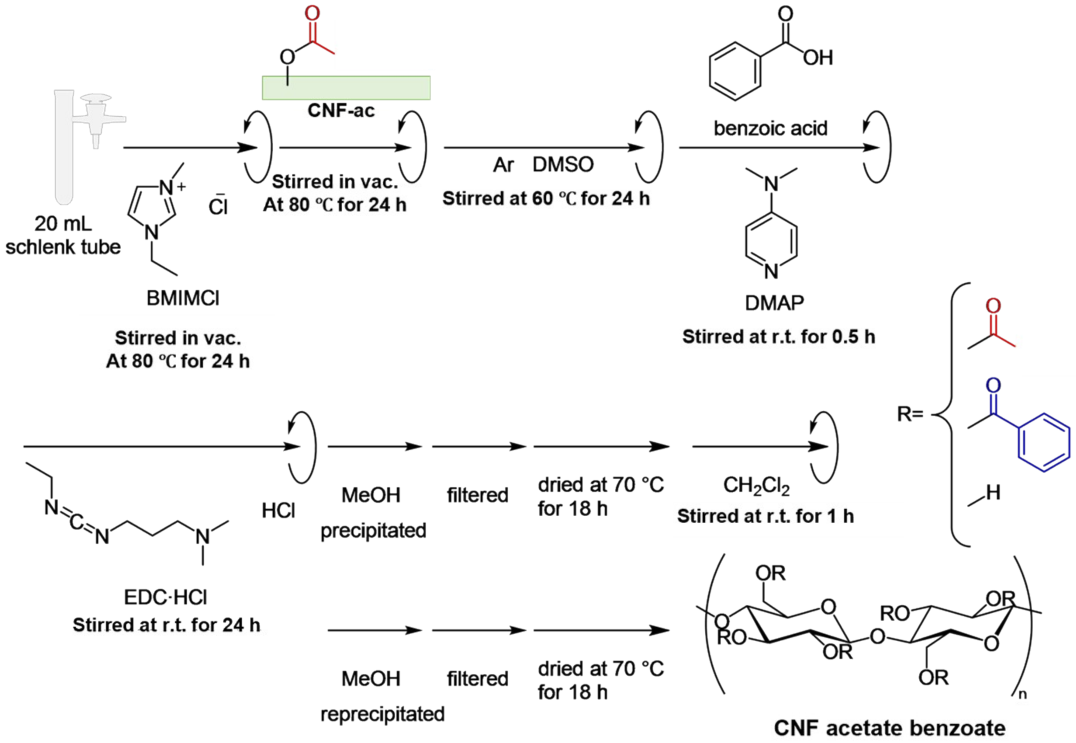

Scheme S1. Benzoylation process of CNF-ac.

First, 0.65 g (10 eq./OH of cellulose) of BMIMCl was added to a Schlenk tube and stirred under vacuum at 80 °C in an oil bath for 24 h. Subsequently, the atmosphere was replaced with Ar, and 20 mg of CNF-ac was added to the Schlenk tube. The mixture was stirred under vacuum at 80 °C in an oil bath for 24 h. Following this, the atmosphere was replaced with Ar again, and 0.58 g (20 eq./OH of cellulose) DMSO was added to the Schlenk tube and stirred at 60 °C for 24 h. Subsequently, 0.14 g (3 eq./OH of cellulose) of benzoic acid and 0.14 g (3 eq. /OH of cellulose) of DMAP were added, and the mixture was stirred at room temperature until complete dissolution. Subsequently, 0.21 g (3 eq./OH of cellulose) of EDC·HCl was added, and the reaction was carried out upon stirring at room temperature for 24 h. The solution was then poured into 20 mL of MeOH to precipitate the product. The product was isolated via vacuum filtration using a nylon membrane filter. The obtained product was dried under vacuum at 70 °C, after which, dichloromethane (1.0 mL) was added to re-dissolve the product. The product was then re-precipitated by pouring it into 10 mL of MeOH and isolated via vacuum filtration using a nylon membrane filter, followed by drying under vacuum at 70 °C to obtain the final product.

To calculate the DS of the products, ^1H NMR spectroscopy was performed in DMSO-d6, and DS was determined from the intensity ratios.

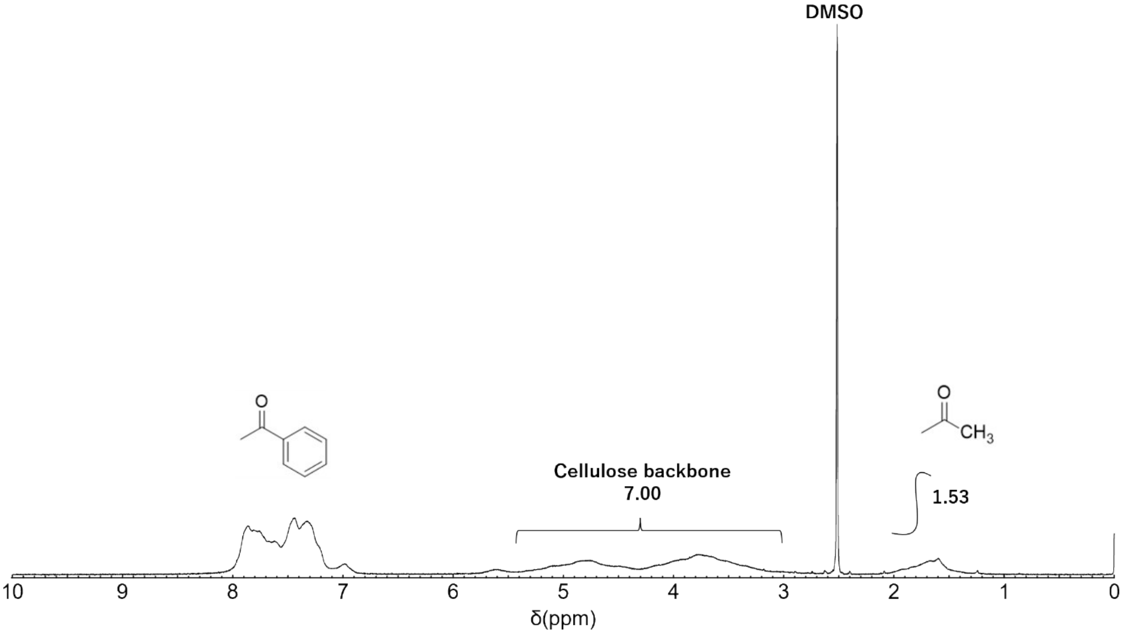

Figure S2. ^1H NMR spectrum (DMSO-d_6) of benzoylated CNF-ac.

The appearance of characteristic aromatic proton signals in the range of 6.9–8.2 ppm confirms the successful benzoylation of CNF-ac. Signals observed at 3.0–5.5 ppm are assigned to protons of the cellulose backbone, whereas resonances in the range 1.5–2.1 ppm correspond to the methyl protons of acetate groups. The acetate methyl protons appear as a broad resonance between 1.5 and 2.2 ppm, which is attributed to the heterogeneous chemical environments of acetyl groups at different substitution sites (C2, C3, and C6) and the co-existence of benzoyl and acetyl substituents along the cellulose backbone.

For DS calculation, the integral of the cellulose backbone region (3.0–5.5 ppm) was normalized to 7 protons per anhydroglucose unit. The DS of the acetate groups was determined by dividing the integrated area of the acetate methyl signal by 3, yielding a DS value of 0.51 based on an integrated area of 1.53.

3. ^1H NMR and ^{13}C NMR spectra for TBA-based salts

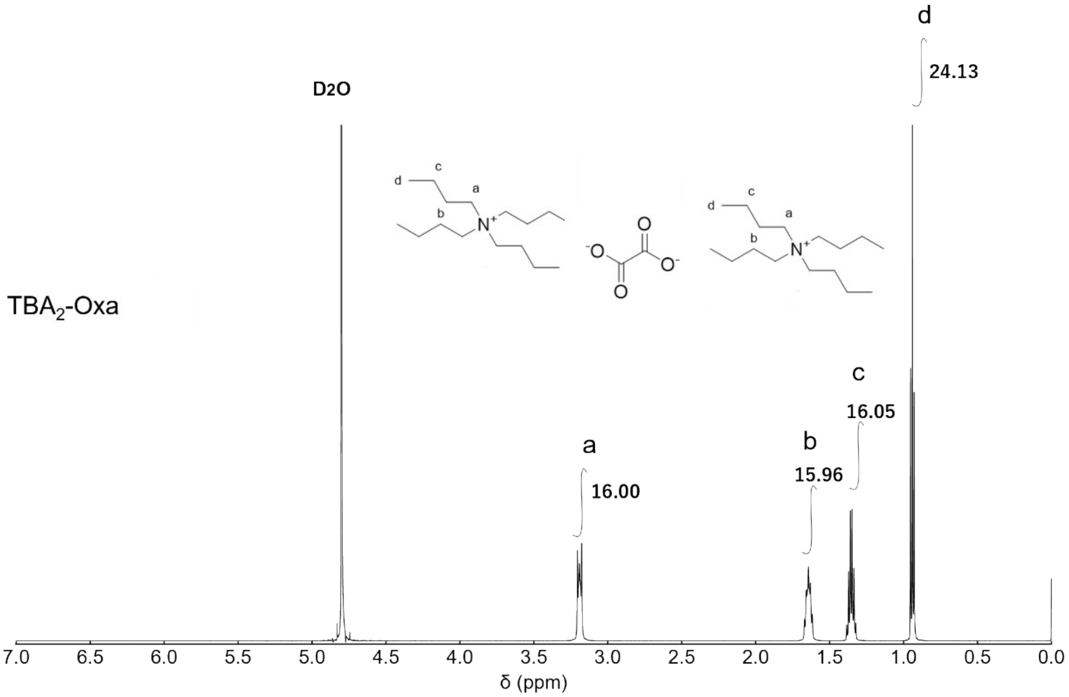

Figure S3. ^{1}H NMR spectra of TBA$_2$-Oxa. δ 3.18–3.20 (m, 8H), 1.59–1.69 (m, 8H), 1.32–1.38 (m, 8H), 0.93–0.95 (t, J ≈ 7.2 Hz, 12H).

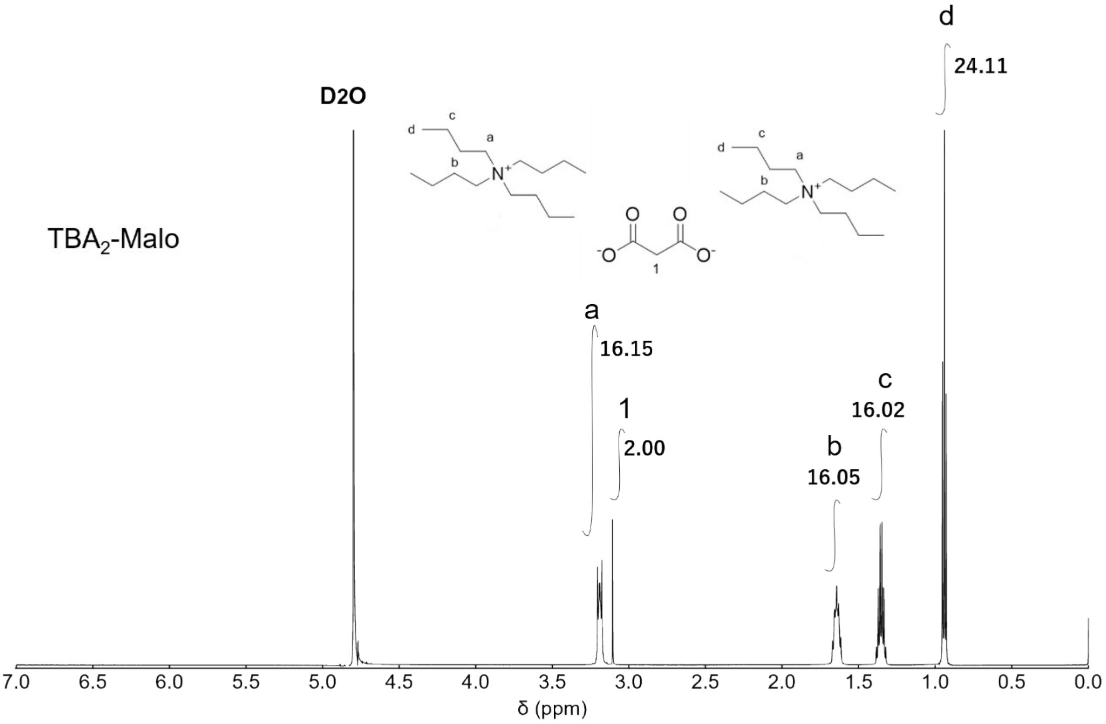

Figure S4. ^{1}H NMR spectra of TBA$_2$-Malo. δ 3.10 (s, 2H), 3.18–3.20 (m, 8H), 1.59–1.69 (m, 8H), 1.32–1.38 (m, 8H), 0.93–0.95 (t, J ≈ 7.2 Hz, 12H).

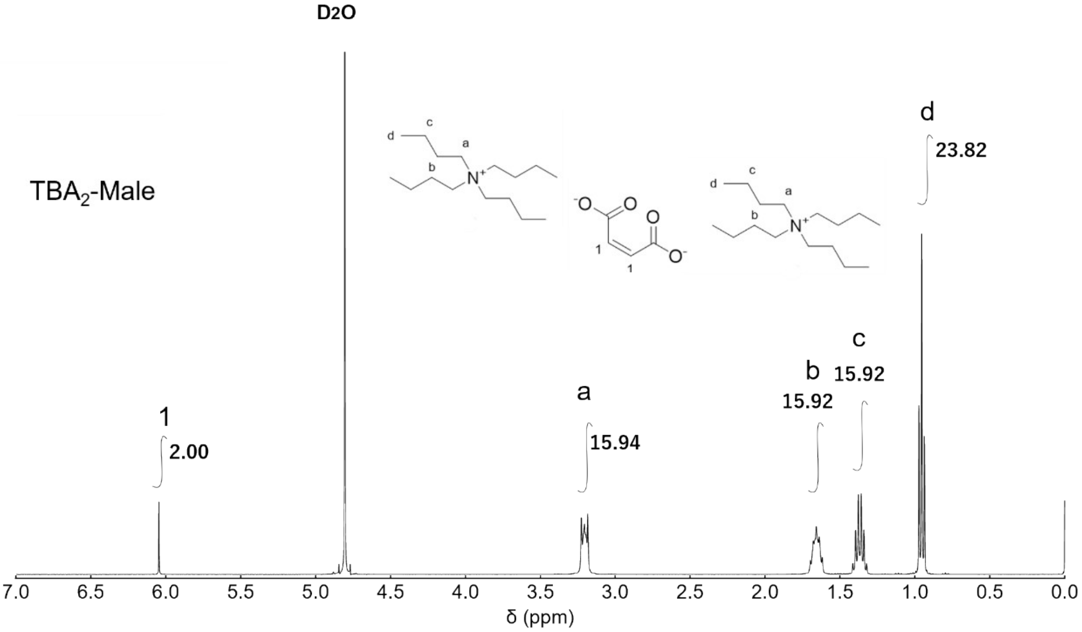

Figure S5. ^{1}H NMR spectra of TBA$_2$-Male. δ 6.05 (d, 2H, cis-CH=CH), 3.18–3.20 (m, 8H), 1.59–1.69 (m, 8H), 1.32–1.38 (m, 8H), 0.93–0.95 (t, J ≈ 7.2 Hz, 12H).

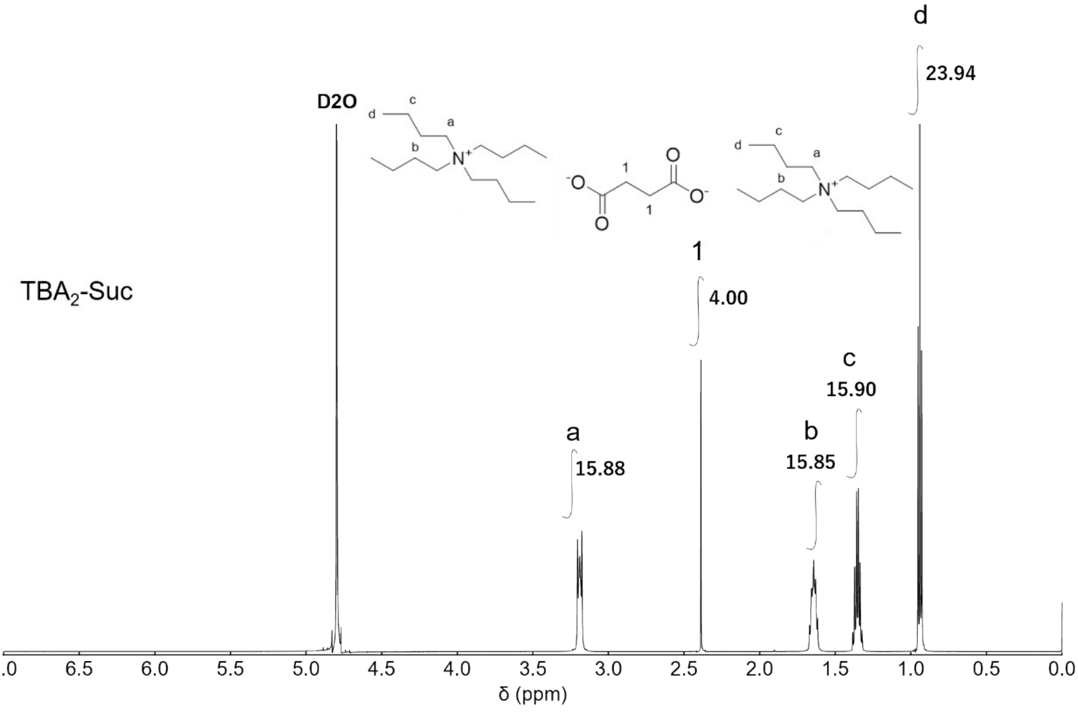

Figure S6. ^{1}H NMR spectra of TBA$_2$-Suc. δ 2.36–2.42 (s, 4H), 3.18–3.20 (m, 8H), 1.59–1.69 (m, 8H), 1.32–1.38 (m, 8H), 0.93–0.95 (t, J ≈ 7.2 Hz, 12H).

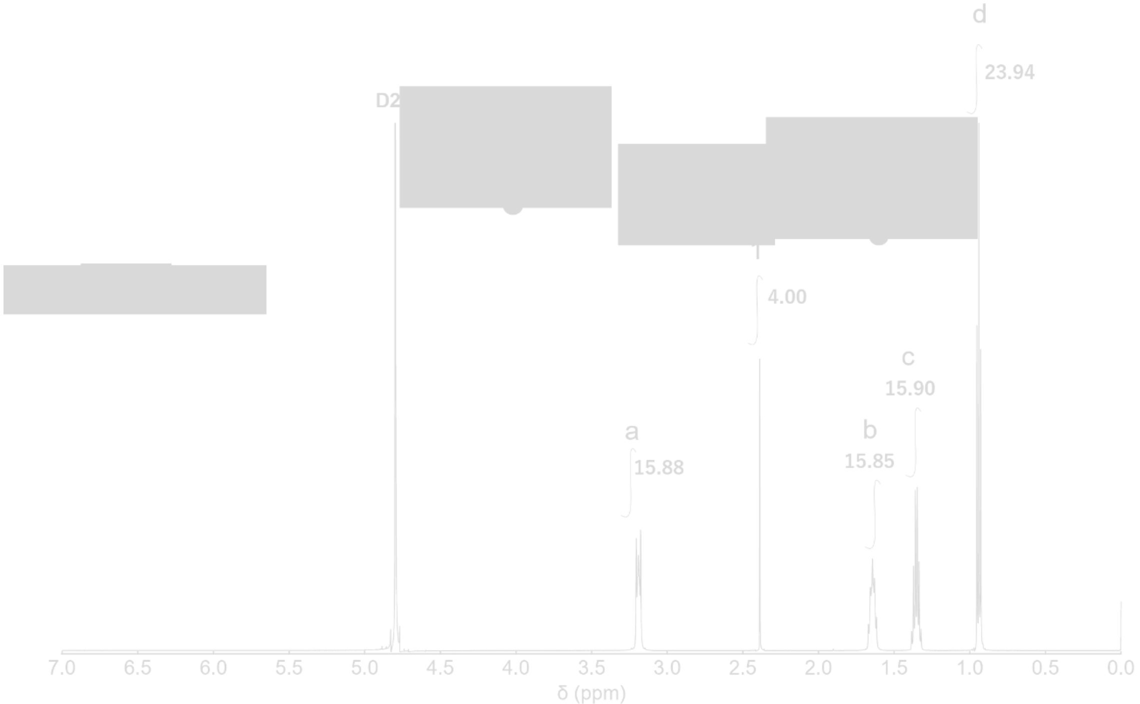

Figure S7. ^{1}H NMR spectra of TBA_2-Fum. δ 6.51 (d, 2H, trans-CH=CH), 3.18–3.20 (m, 8H), 1.59–1.69 (m, 8H), 1.32–1.38 (m, 8H), 0.93–0.95 (t, J ≈ 7.2 Hz, 12H).

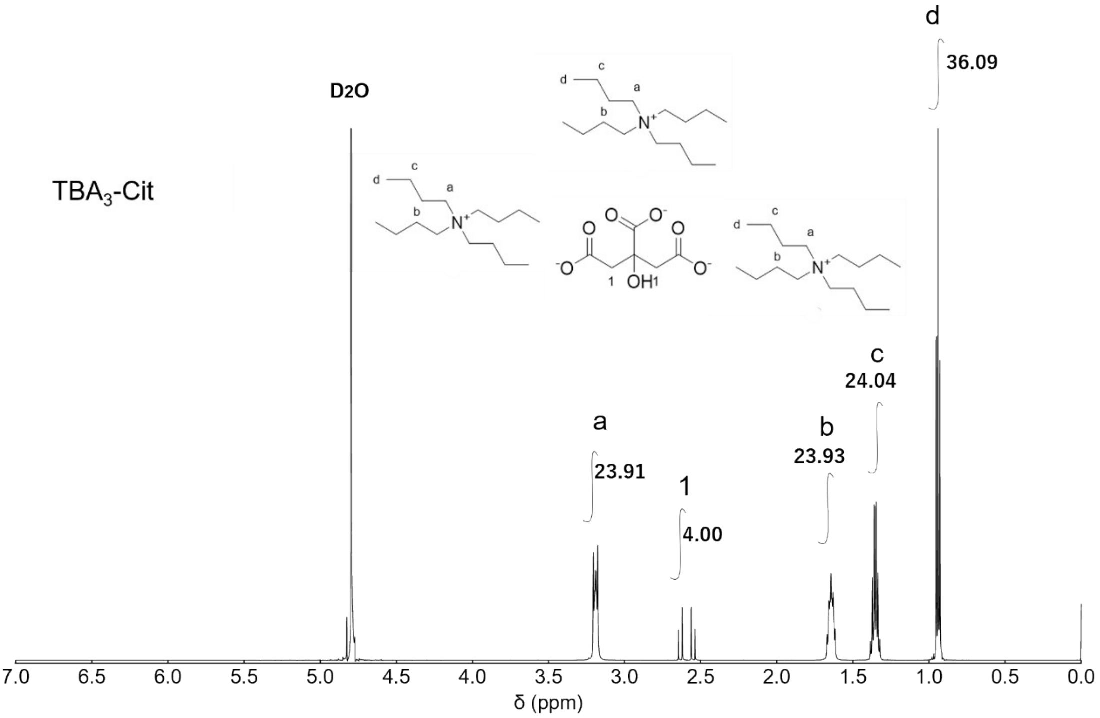

Figure S8. ^{1}H NMR spectra of TBA_2-Cit. δ 2.62–2.65 (dd, J = 15.0 Hz, 4H), 3.18–3.20 (m, 8H), 1.59–1.69 (m, 8H), 1.32–1.38 (m, 8H), 0.93–0.95 (t, J ≈ 7.2 Hz, 12H).

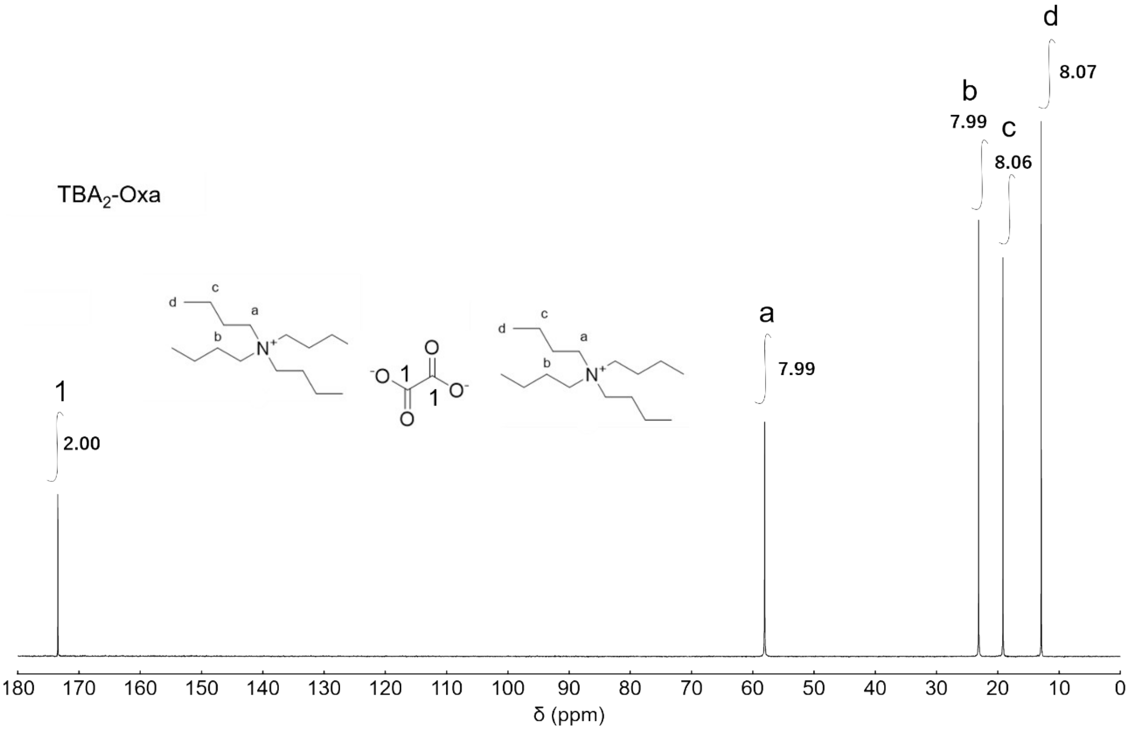

Figure S9. ^{13}C NMR spectra of TBA_2-Oxa. δ 173.46, 57.95, 23.25, 19.24, 12.67.

Based on these ^{1}H NMR results and ^{13}C NM R data, the obtained products were the desired tetrabutylammonium salts.

4. Polarized optical microscopy images

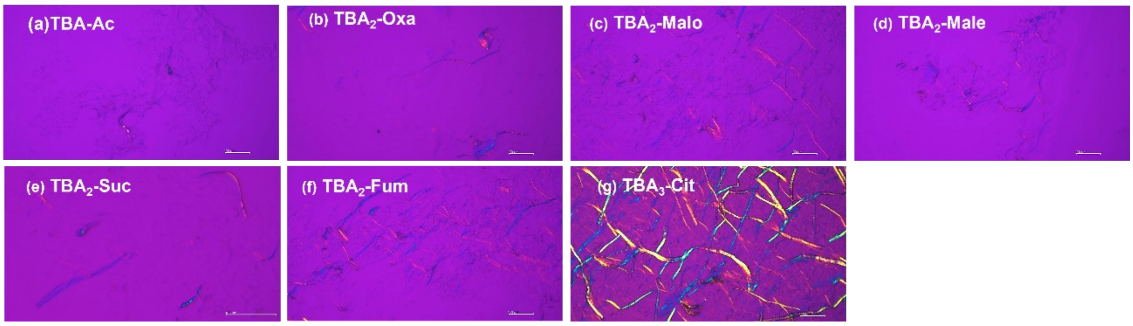

Figure S10. Polarized optical microscopy images of CNFs after 3 h of redispersion in 7 different TBA-salt/DMSO solvent systems.

5. XRD result of CNF-ac

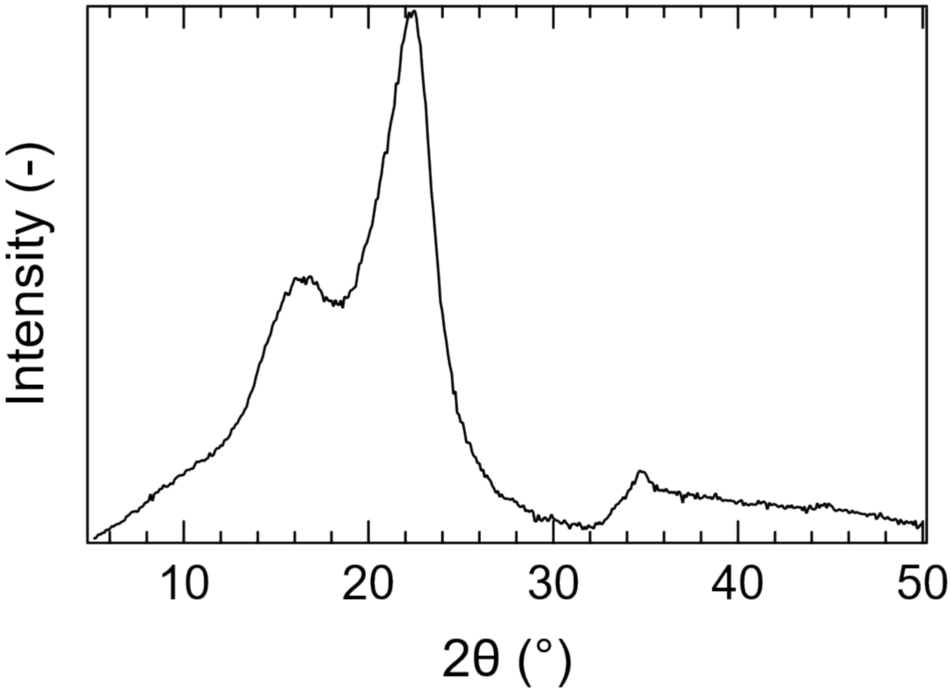

Figure S11. XRD pattern of surface-modified bamboo CNF-ac.

The XRD pattern of CNF-ac confirms that the cellulose I crystallinity is retained after surface acetylation. This is because the mixed solvent system composed of TBA_2-Male, DMSO, and CH_3CN is insufficient to fully dissolve bamboo-derived cellulose nanofibers. Consequently, acetylation occurs primarily at the fiber surface rather than through bulk dissolution, leaving the internal crystalline domains intact and allowing the native cellulose I structure to remain unchanged.

6. Images of reinforced membranes

A comparative study was conducted on hot-pressed films fabricated by blending commercial cellulose acetate (CA) with acetylated bamboo cellulose nanofibrils (CNF-ac, 1, 3, and 5 wt%) and unmodified bamboo CNF (1, 3, and 5 wt%). Visual inspection revealed distinct morphological differences between the two groups. Films containing unmodified CNF exhibited macroscopic phase separation with aggregated structures, whereas the CNF-ac/CA composites demonstrated homogeneous dispersion across all concentrations. As shown in Fig. S12, representative images of the 5 wt% formulations highlight this contrast: the CNF-ac/CA film (Fig. S12a) maintained optical uniformity, whereas the unmodified CNF/CA film (Fig. S12b) displayed conspicuous condensates. This phenomenon suggests that acetylation effectively improves the interfacial compatibility between bamboo CNFs and the CA matrix, likely through enhanced hydrophobic interactions and reduced hydrogen-bonding propensity in CNF-ac.

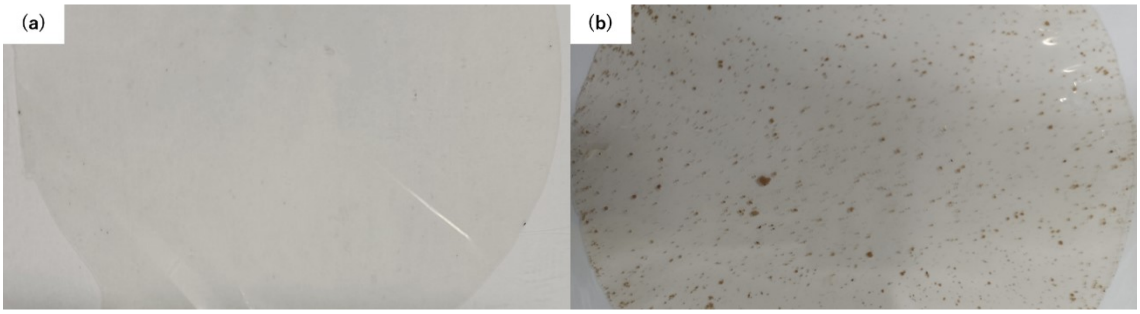

Figure S12. Digital images of the reinforced membranes with (a) 5 wt% CNF-ac and (b) 5 wt% CNF.

The results indicated that CNF-ac exhibited better compatibility with CA than the unmodified CNFs. No visible agglomeration was observed, and CNF-ac was uniformly dispersed within the CA matrix. In contrast, the unmodified CNFs showed noticeable agglomeration, which was further confirmed microscopically.

7. Mechanical properties of reinforced films

Fig. S13 presents the stress–strain curves of hot-pressed plasticizer-containing CA/bamboo CNF composite films with different CNF contents. Compared with the pure CA film (0 wt%), the addition of CNFs significantly increased the tensile strength, indicating that the CNFs act as a reinforcing phase within the matrix. However, this improvement in strength is accompanied by a reduction in elongation at break, particularly at higher CNF contents (3 and 5 wt%), suggesting that CNFs restrict polymer chain mobility and consequently reduce film ductility.

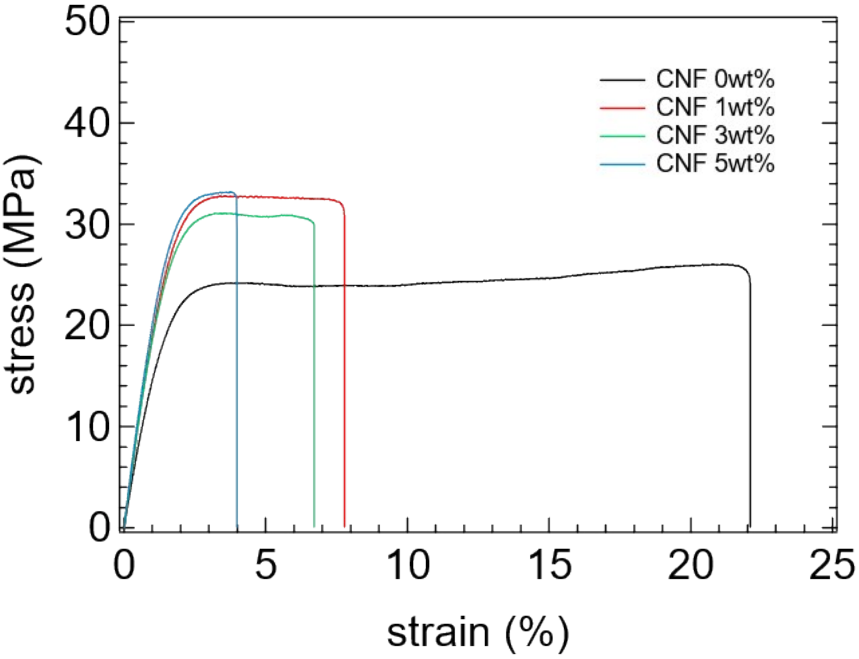

Figure S13. Stress-strain curve of cellulose acetate films reinforced with unmodified CNFs.

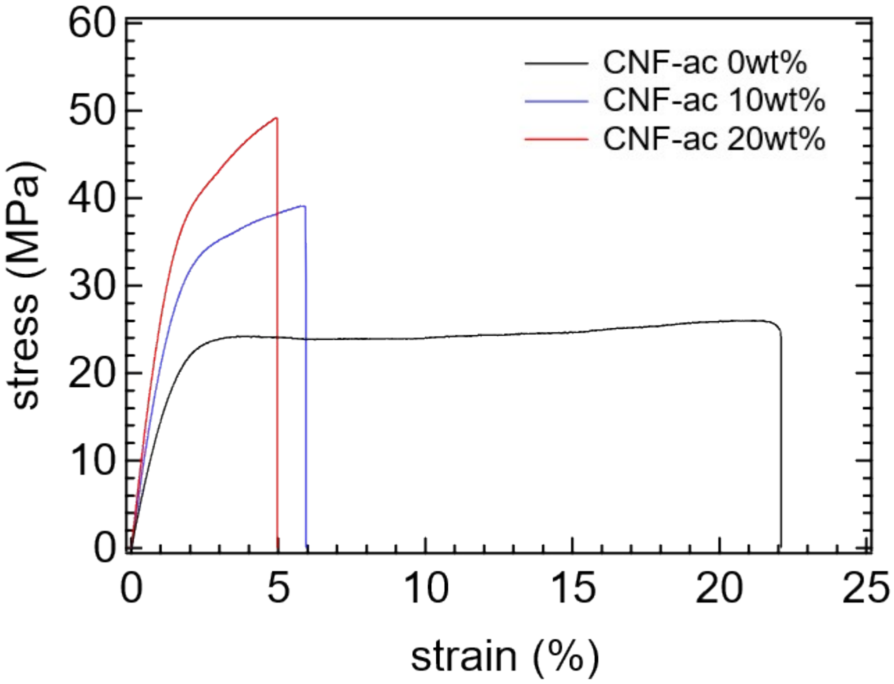

Figure S14. Stress-strain curve of cellulose acetate films reinforced with 10 and 20 wt% CNF-ac.

At higher CNF-ac loadings of 10 and 20 wt%, a further increase in tensile strength was observed, reaching 38.9 and 49.19 MPa, respectively. However, this improvement in strength was accompanied by a reduction in elongation at break. Specifically, the elongation decreased to approximately 5.81% at 10 wt% CNF-ac and further declined to 4.95% at 20 wt%. The SS curve is shown in Fig. S14. Moreover, control samples containing 10 and 20 wt% unmodified bamboo CNFs exhibited severe fiber aggregation, which prevented the formation of films suitable for tensile test, thereby precluding a meaningful comparison. For these reasons, the tensile properties at 10 and 20 wt% CNF-ac are provided only in the SI.